**Supplementary information**

Carn, S. A., Fioletov, V., McLinden, C., Li, C. & Krotkov, N. A.

A decade of global volcanic $SO_2$ emissions measured from space. *Sci. Rep*.

Supplementary Table 1

The complete volcanic $SO_2$ emissions inventory is provided as an Excel spreadsheet, including annual $SO_2$ emissions and 1σ emission uncertainties for each volcanic source, and statistics from a weighted linear regression fit to the annual mean $SO_2$ emissions.

Supplementary Figures

The following figures show a global map of the volcanic $SO_2$ sources (Fig. S1), regional maps of some volcanic $SO_2$ sources (Figs. S2-S8), and time-series plots of annual mean $SO_2$ fluxes for 2005-2015 for the volcanic sources ranked 11-91 in the volcanic $SO_2$ emissions inventory (Figs. S9-S16).

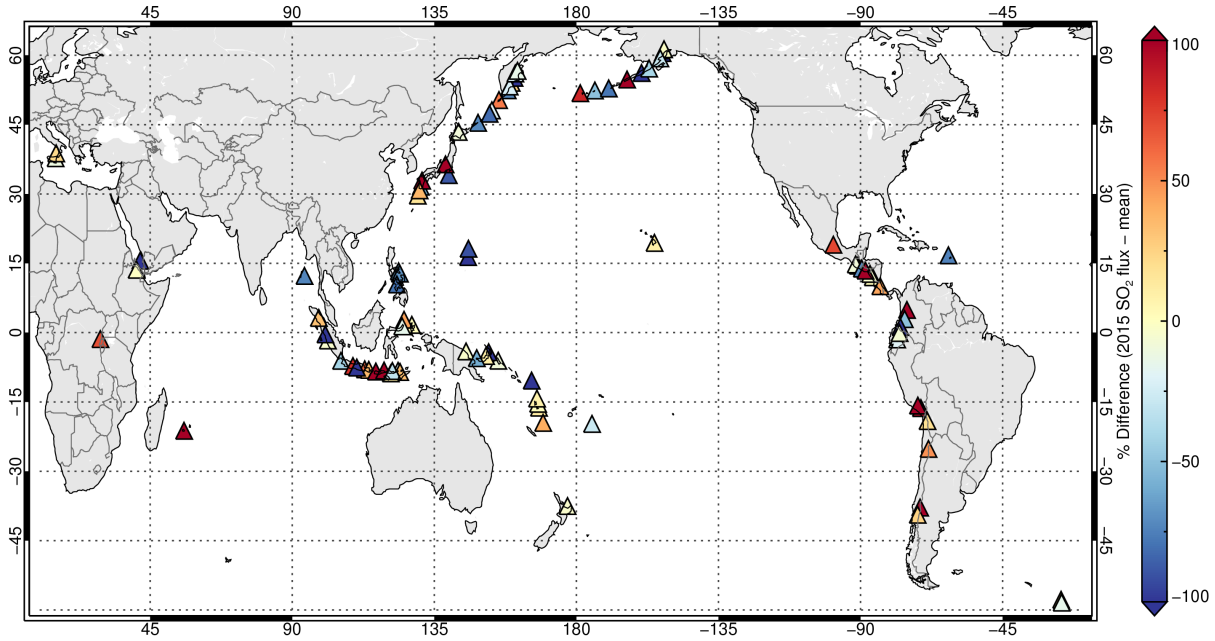


**Figure S1.** Global map of 91 volcanic $SO_2$ sources (*triangles*) in the OMI-derived $SO_2$ emissions inventory. Sources are colored based on the % difference between their annual mean $SO_2$ emissions in 2015 and their 2005-2015 decadal mean $SO_2$ flux. Hence, warm and cold colors indicate sources with 2015 $SO_2$ emissions above and below the long-term average, respectively. More detailed regional maps of the volcanic $SO_2$ sources are provided in Figures S2-S8. Map generated using Interactive Data Language (IDL) version 8.5.1 (http://www.harrisgeospatial.com/).

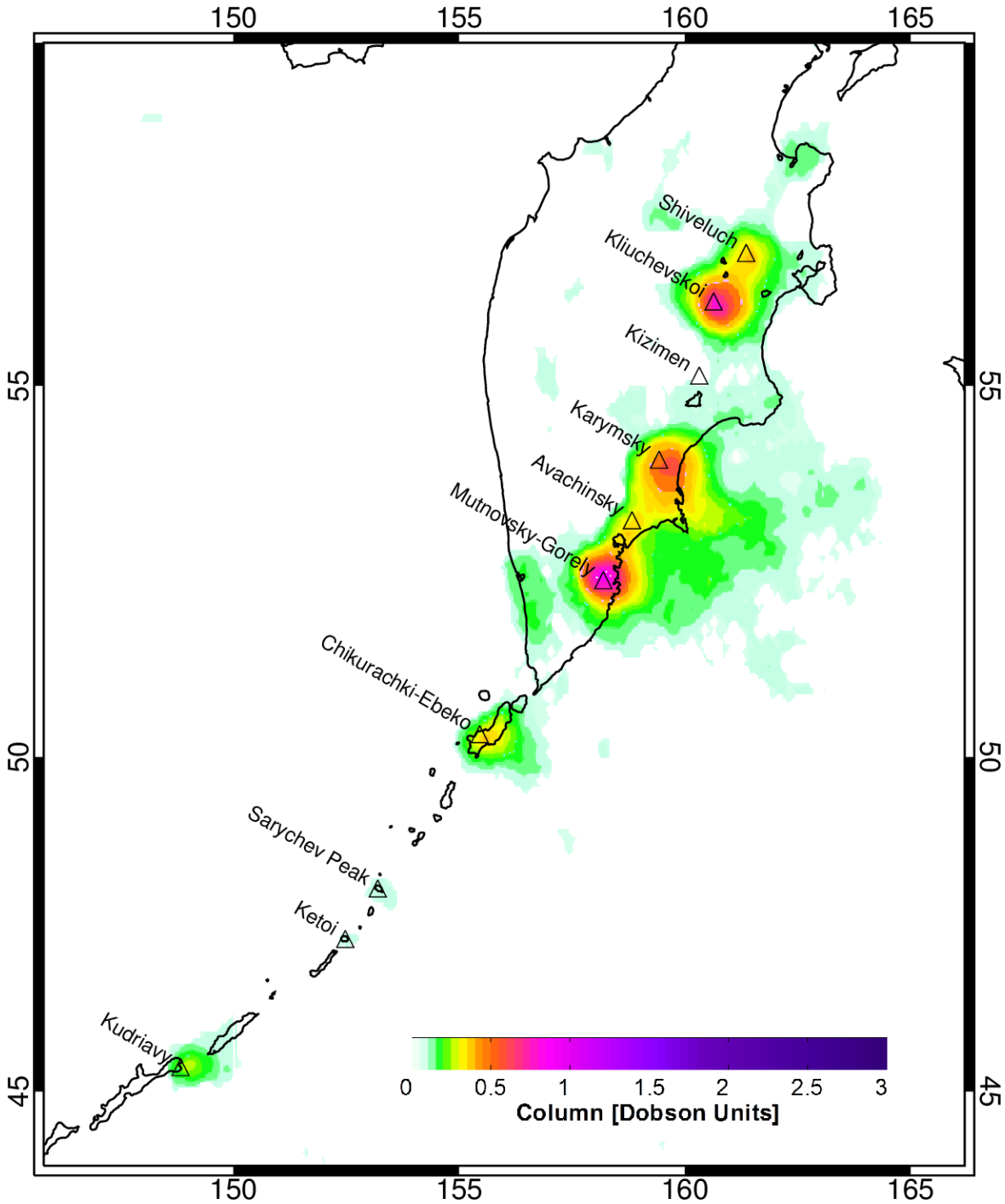


**Figure S2.** Mean OMI $SO_2$ columns (in Dobson Units [DU]; 1 DU = $2.69\times10^{16}$ molecules $cm^{-2}$) for 2005-2007 over Kamchatka and the Kuril Islands (Russia). The volcanic $SO_2$ sources (including paired sources) responsible for the observed $SO_2$ emissions are labeled. The absence of an $SO_2$ anomaly (e.g., at Kizimen) indicates either that the volcano was not active in 2005-2007 or that its emissions were below detection limits. Map generated using IDL version 8.5.1 (http://www.harrisgeospatial.com/).

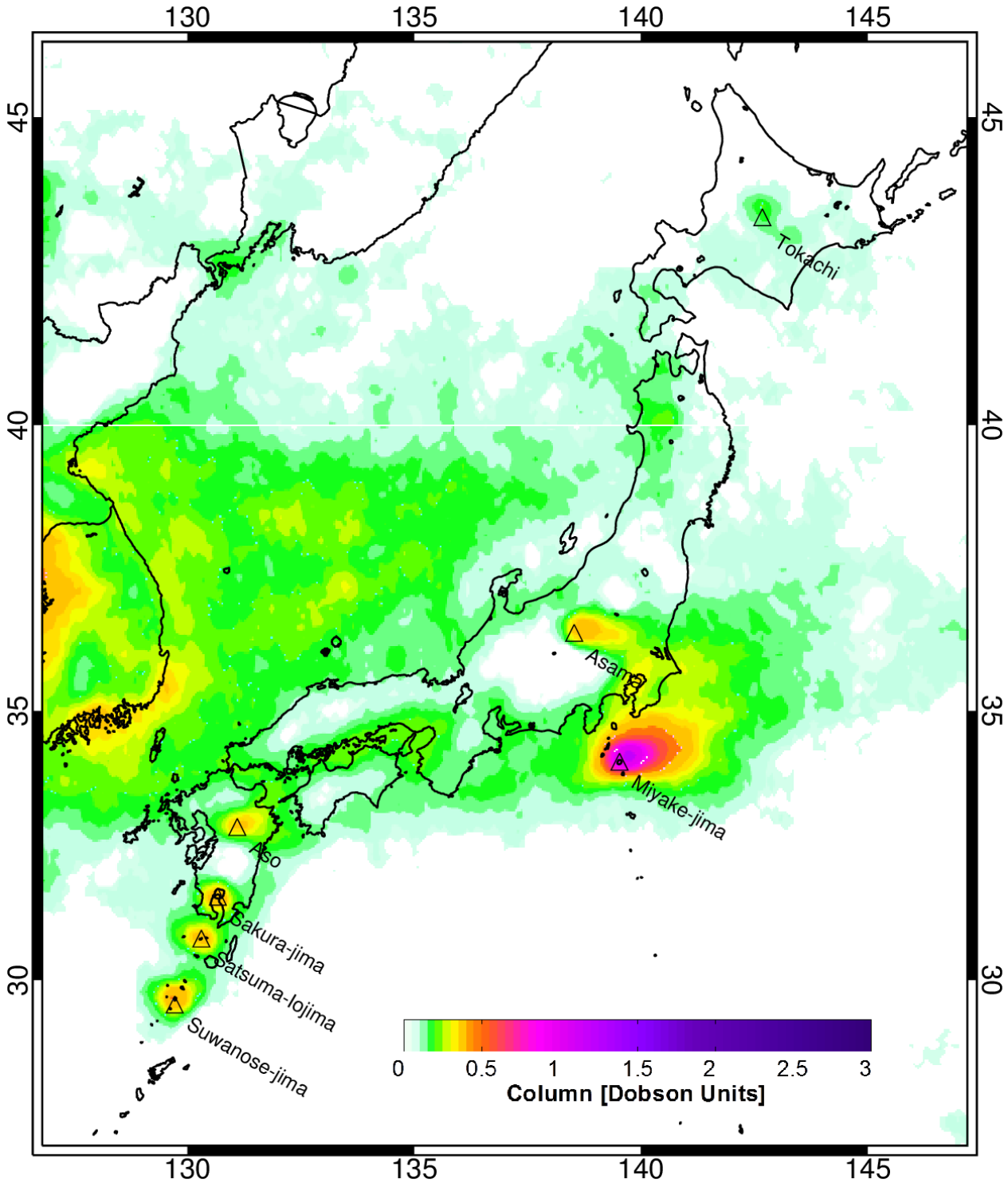


**Figure S3.** Mean OMI $SO_2$ columns (DU) for 2005-2007 over Japan. The volcanic $SO_2$ sources responsible for the observed $SO_2$ emissions are labeled. Elevated $SO_2$ columns to the west of Japan are derived from anthropogenic pollution in China. Map generated using IDL version 8.5.1 (http://www.harrisgeospatial.com/).

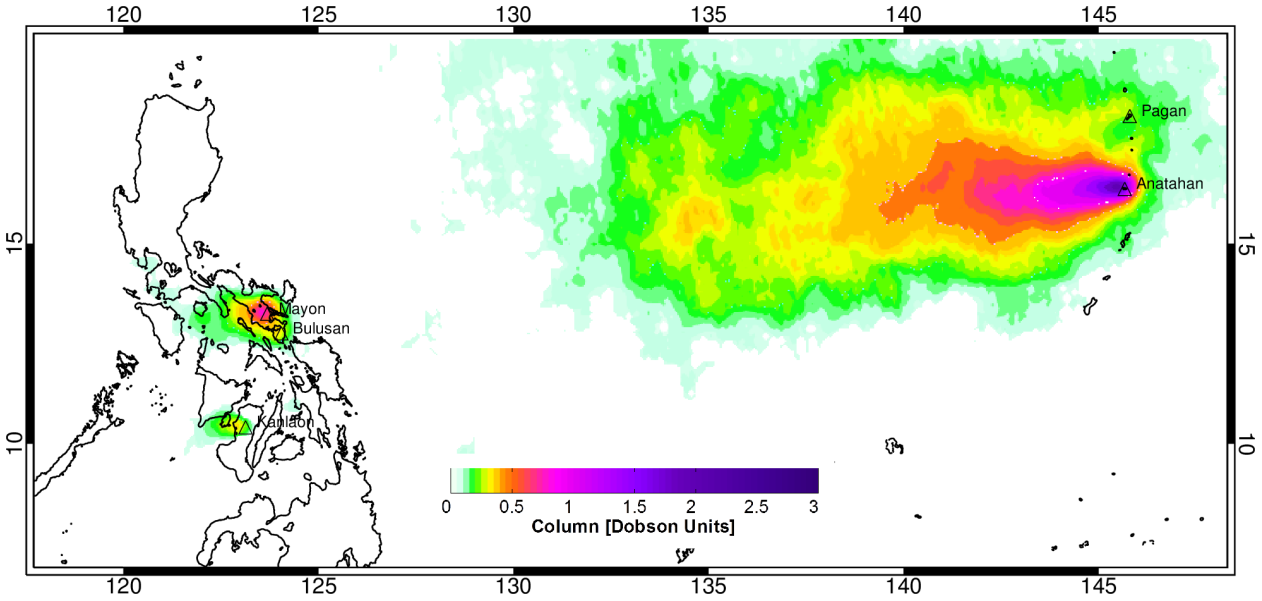


**Figure S4.** Mean OMI $SO_2$ columns (DU) for 2005-2007 over the Philippines and the Commonwealth of the Northern Mariana Islands (CNMI, USA). The volcanic $SO_2$ sources responsible for the observed $SO_2$ emissions are labeled. Map generated using IDL version 8.5.1 (http://www.harrisgeospatial.com/).

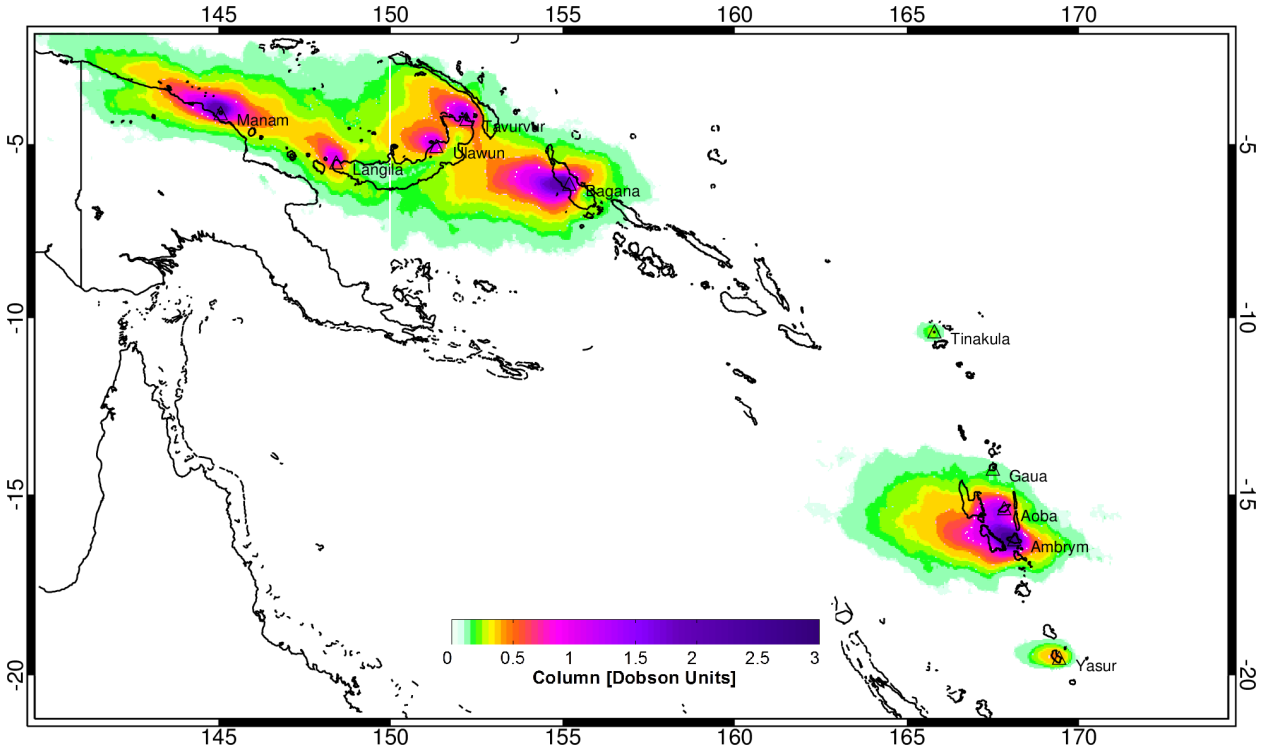


**Figure S5.** Mean OMI $SO_2$ columns (DU) for 2005-2007 over Papua New Guinea, the Solomon Islands and Vanuatu. The volcanic $SO_2$ sources responsible for the observed $SO_2$ emissions are labeled. Map generated using IDL version 8.5.1 (http://www.harrisgeospatial.com/).

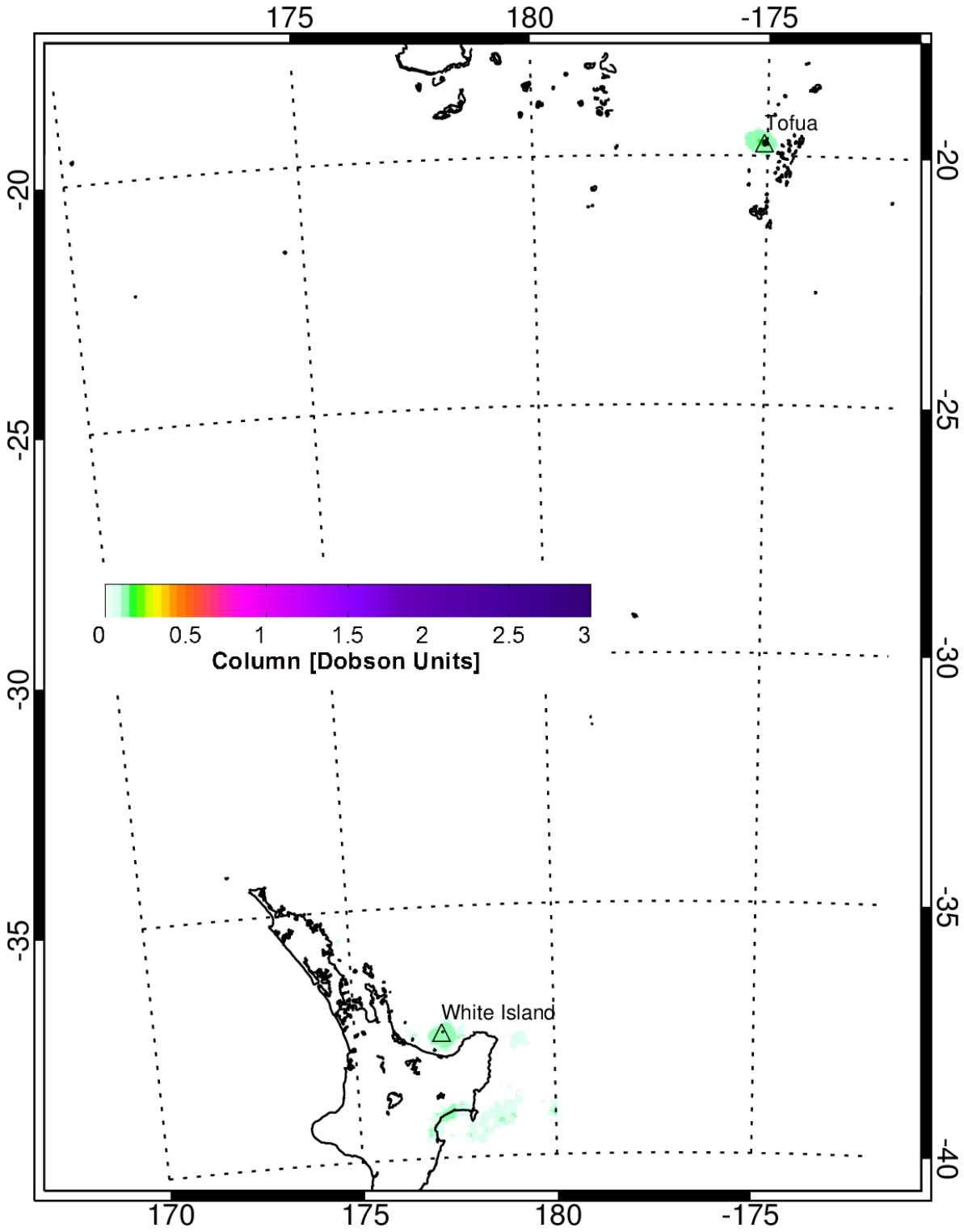


**Figure S6.** Mean OMI $SO_2$ columns (DU) for 2005-2007 over New Zealand and Tonga. The volcanic $SO_2$ sources responsible for the observed $SO_2$ emissions are labeled. Map generated using IDL version 8.5.1 (http://www.harrisgeospatial.com/).

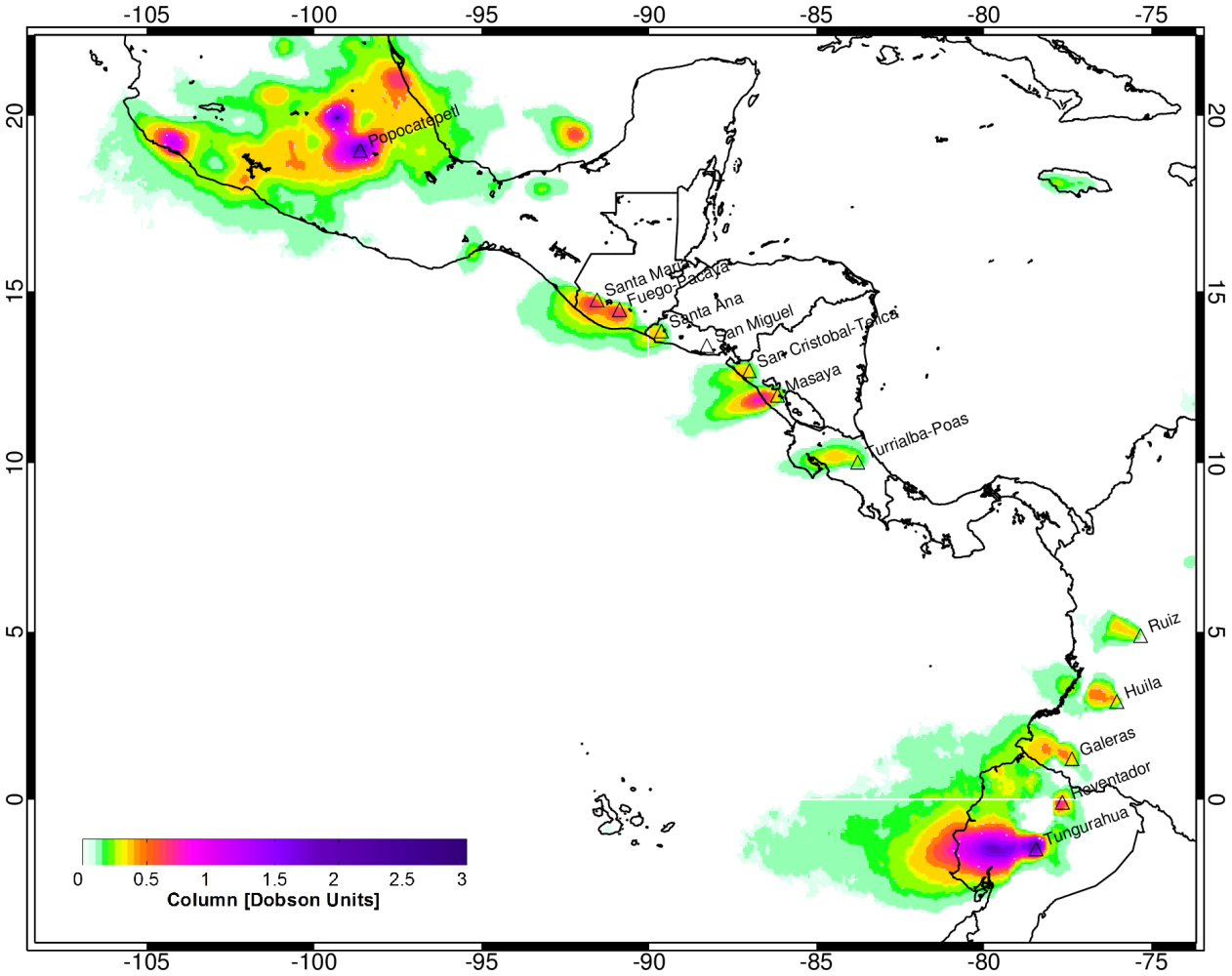


**Figure S7.** Mean OMI $SO_2$ columns (DU) for 2005-2007 over Mexico, Guatemala, El Salvador, Nicaragua, Costa Rica, Colombia and Ecuador. The volcanic $SO_2$ sources (including paired sources) responsible for the observed $SO_2$ emissions are labeled. Anthropogenic $SO_2$ sources in Mexico are also apparent. Map generated using IDL version 8.5.1 (http://www.harrisgeospatial.com/).

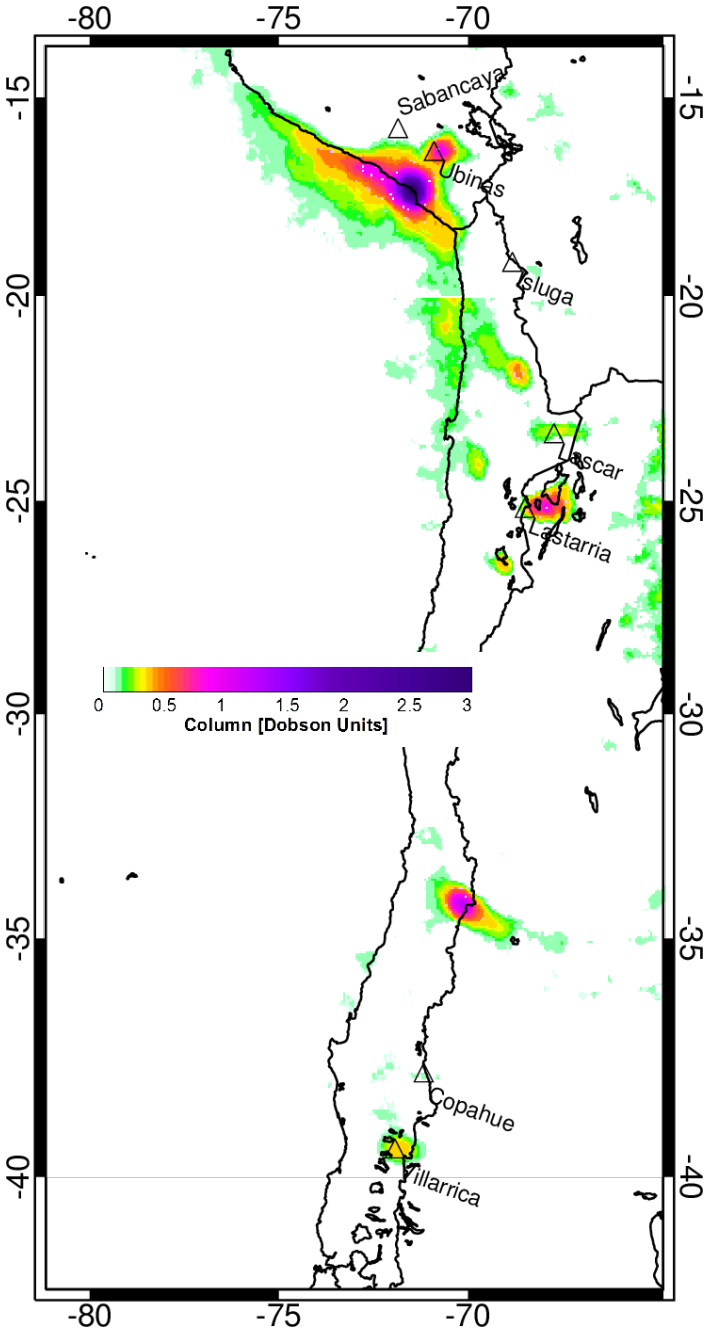


**Figure S8.** Mean OMI $SO_2$ columns (DU) for 2005-2007 over Peru, Chile and Argentina. The volcanic $SO_2$ sources responsible for the observed $SO_2$ emissions are labeled. Anthropogenic $SO_2$ sources in Peru and Chile are also apparent. The absence of an $SO_2$ anomaly (e.g., at Sabancaya) indicates either that the volcano was not active in 2005-2007 or that its emissions were below detection limits. A possible $SO_2$ signal is associated with Lascar, but this volcano is not included in the emissions inventory. Map generated using IDL version 8.5.1 (http://www.harrisgeospatial.com/).

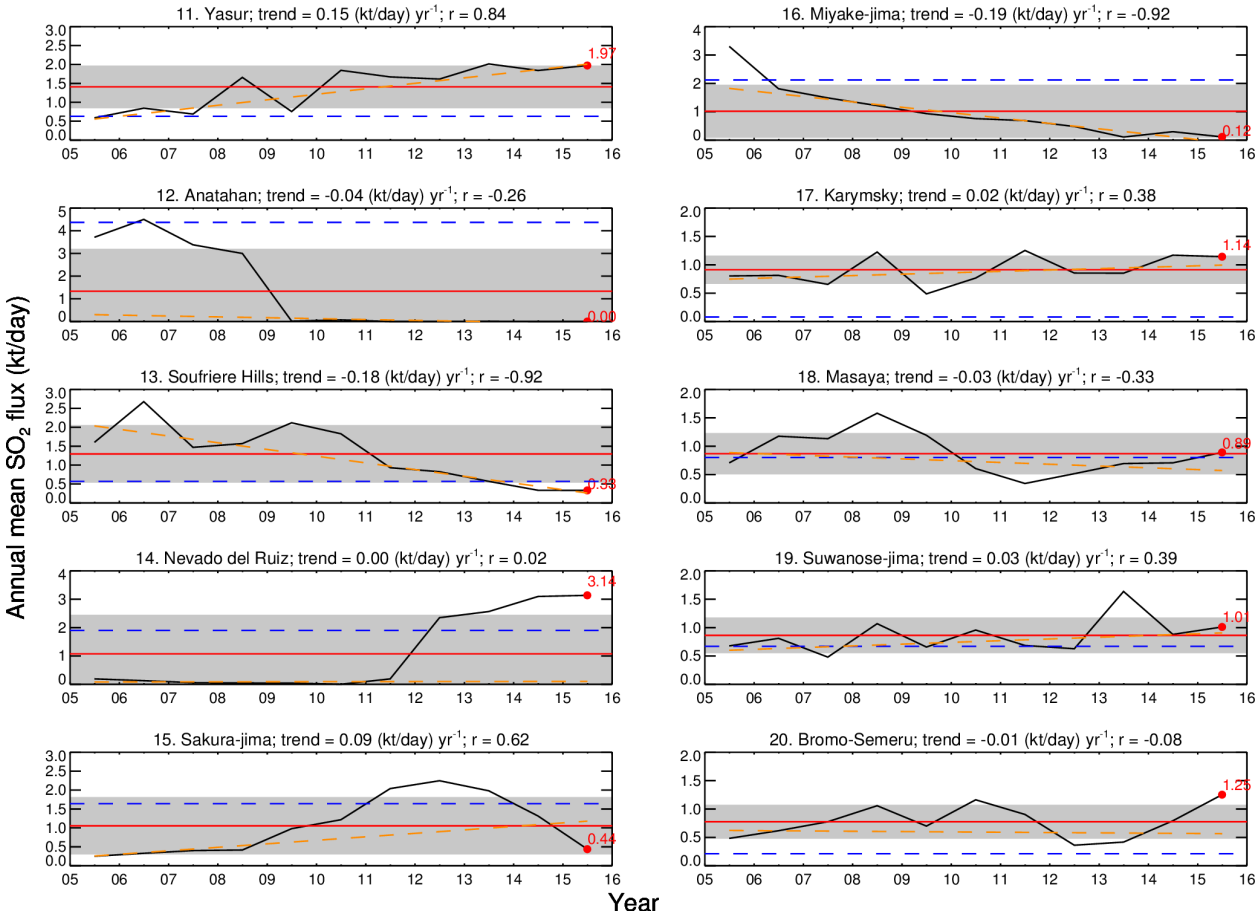


**Figure S9.** OMI-derived annual mean $SO_2$ fluxes in 2005-2015 for the volcanic $SO_2$ sources ranked 11-20 in the inventory. Plots are titled with the volcanic source name and rank, and the trend (slope) and linear correlation coefficient (*r*) of an error-weighted linear regression fit of the annual mean $SO_2$ fluxes. Each plot shows the annual mean $SO_2$ fluxes (*solid black line*), mean $SO_2$ flux in 2015 (*labeled red dot*), linear regression trend line (*dashed orange line*), decadal mean $SO_2$ flux (*horizontal red line*), ±1 standard deviation of the decadal mean $SO_2$ flux (*gray band*), and an independent estimate of $SO_2$ flux (*horizontal dashed blue line*) from a recent compilation[1] or another source. If the latter is not available, the plot is labeled with 'N/A'. Here, independent $SO_2$ flux data for Anatahan and Bromo-Semeru are from [2] – [4].

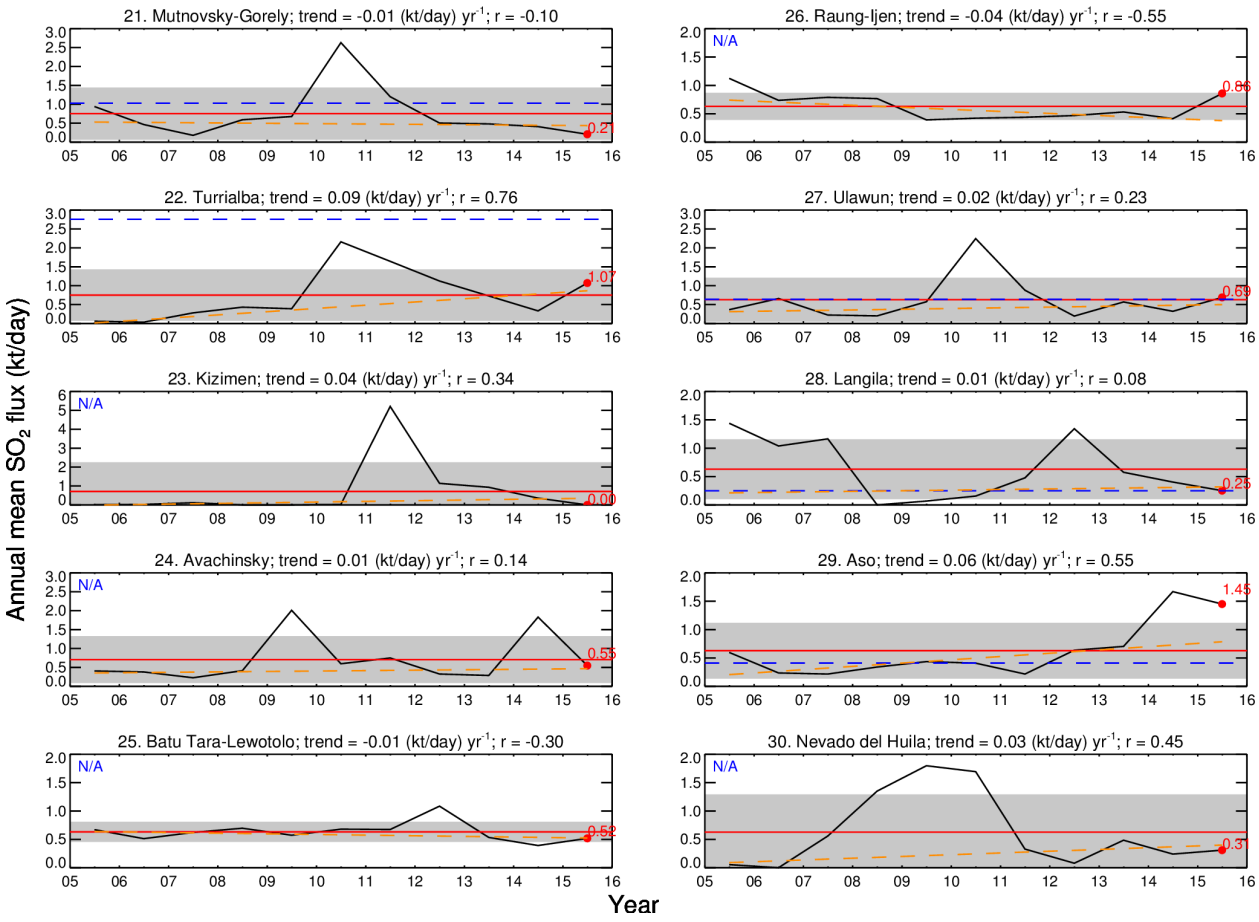


**Figure S10.** OMI-derived annual mean $SO_2$ fluxes in 2005-2015 for the volcanic $SO_2$ sources ranked 21-30 in the inventory. Plots are titled with the volcanic source name and rank, and the trend (slope) and linear correlation coefficient (*r*) of an error-weighted linear regression fit of the annual mean $SO_2$ fluxes. Each plot shows the annual mean $SO_2$ fluxes (*solid black line*), mean $SO_2$ flux in 2015 (*labeled red dot*), linear regression trend line (*dashed orange line*), decadal mean $SO_2$ flux (*horizontal red line*), ±1 standard deviation of the decadal mean $SO_2$ flux (*gray band*), and an independent estimate of $SO_2$ flux (*horizontal dashed blue line*) from a recent compilation[1] or another source. If the latter is not available, the plot is labeled with 'N/A'. Here, independent $SO_2$ flux data for Turrialba are from [5].

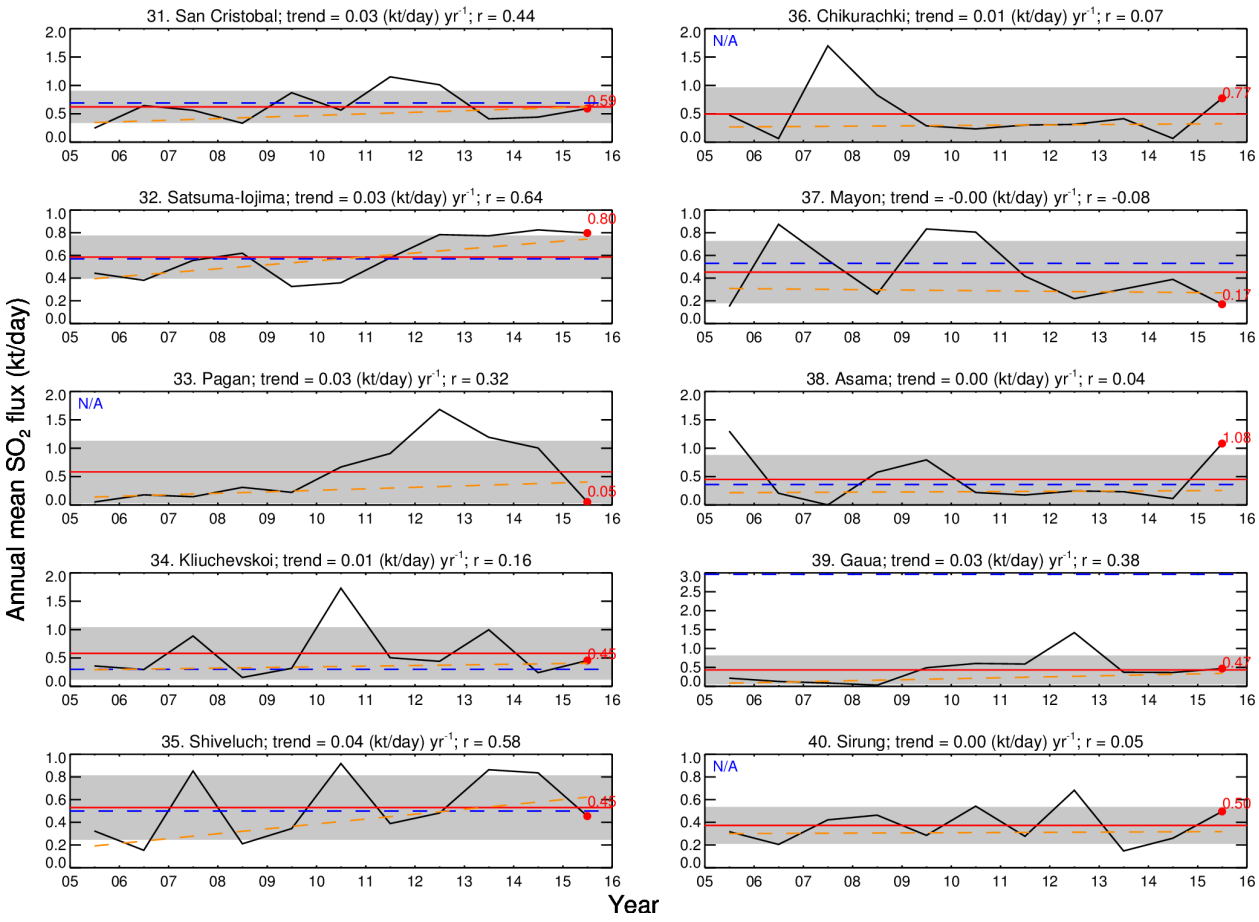


**Figure S11.** OMI-derived annual mean $SO_2$ fluxes in 2005-2015 for the volcanic $SO_2$ sources ranked 31-40 in the inventory. Plots are titled with the volcanic source name and rank, and the trend (slope) and linear correlation coefficient (*r*) of an error-weighted linear regression fit of the annual mean $SO_2$ fluxes. Each plot shows the annual mean $SO_2$ fluxes (*solid black line*), mean $SO_2$ flux in 2015 (*labeled red dot*), linear regression trend line (*dashed orange line*), decadal mean $SO_2$ flux (*horizontal red line*), ±1 standard deviation of the decadal mean $SO_2$ flux (*gray band*), and an independent estimate of $SO_2$ flux (*horizontal dashed blue line*) from a recent compilation[1] or another source. If the latter is not available, the plot is labeled with 'N/A'. Here, independent $SO_2$ flux data for Gaua are from [6].

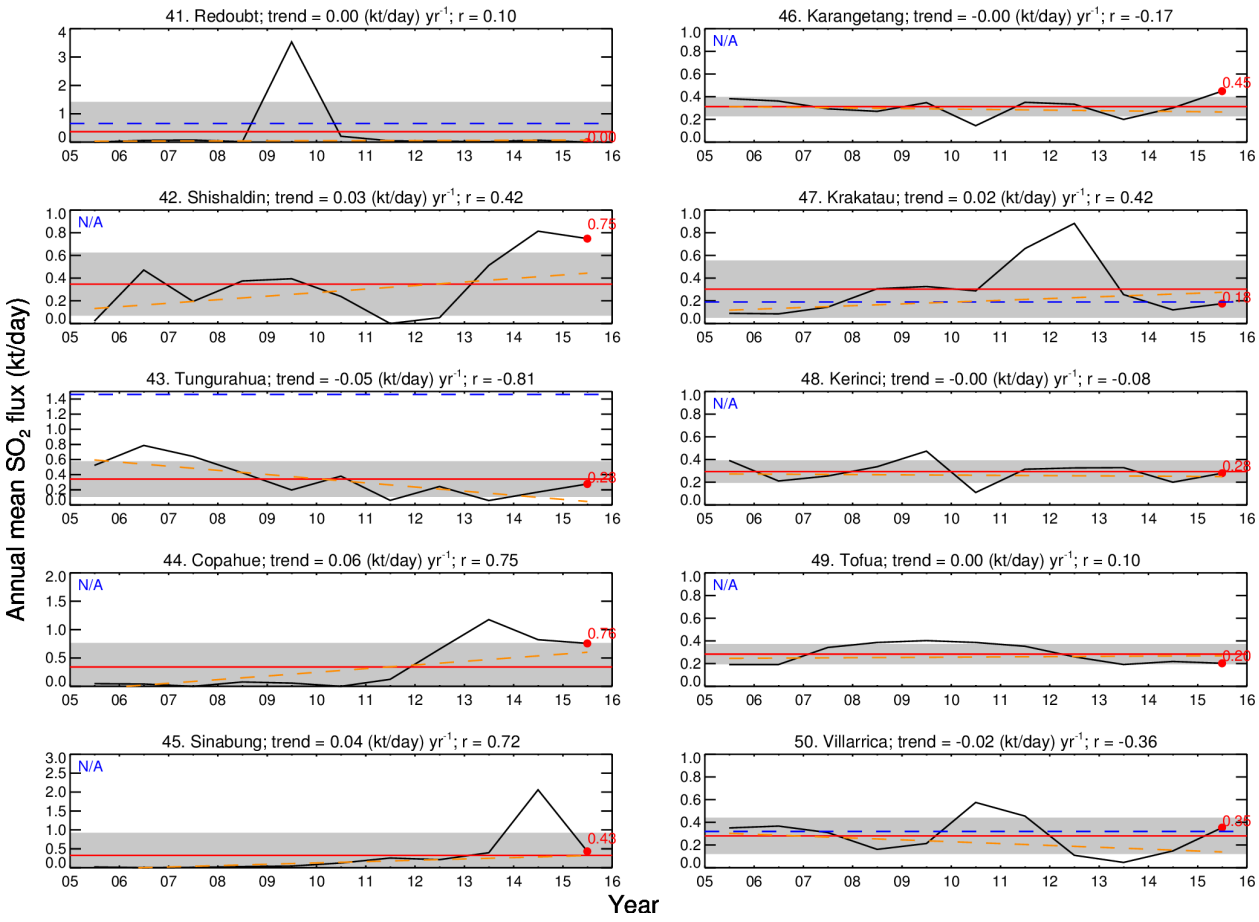


**Figure S12.** OMI-derived annual mean $SO_2$ fluxes in 2005-2015 for the volcanic $SO_2$ sources ranked 41-50 in the inventory. Plots are titled with the volcanic source name and rank, and the trend (slope) and linear correlation coefficient (*r*) of an error-weighted linear regression fit of the annual mean $SO_2$ fluxes. Each plot shows the annual mean $SO_2$ fluxes (*solid black line*), mean $SO_2$ flux in 2015 (*labeled red dot*), linear regression trend line (*dashed orange line*), decadal mean $SO_2$ flux (*horizontal red line*), ±1 standard deviation of the decadal mean $SO_2$ flux (*gray band*), and an independent estimate of $SO_2$ flux (*horizontal dashed blue line*) from a recent compilation[1] or another source. If the latter is not available, the plot is labeled with 'N/A'. Here, independent $SO_2$ flux data for Redoubt and Krakatau are from [7] and [8], respectively.

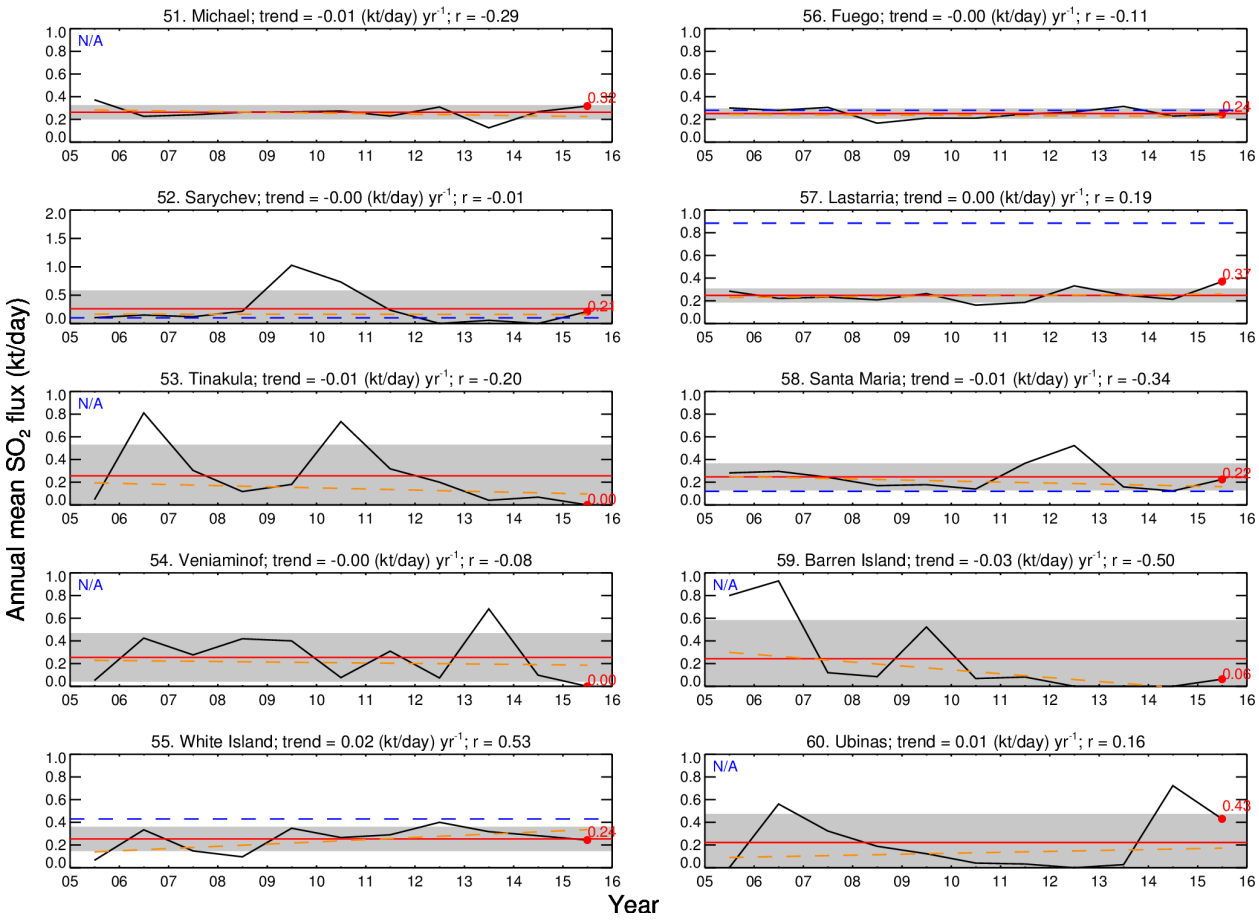


**Figure S13.** OMI-derived annual mean $SO_2$ fluxes in 2005-2015 for the volcanic $SO_2$ sources ranked 51-60 in the inventory. Plots are titled with the volcanic source name and rank, and the trend (slope) and linear correlation coefficient (*r*) of an error-weighted linear regression fit of the annual mean $SO_2$ fluxes. Each plot shows the annual mean $SO_2$ fluxes (*solid black line*), mean $SO_2$ flux in 2015 (*labeled red dot*), linear regression trend line (*dashed orange line*), decadal mean $SO_2$ flux (*horizontal red line*), ±1 standard deviation of the decadal mean $SO_2$ flux (*gray band*), and an independent estimate of $SO_2$ flux (*horizontal dashed blue line*) from a recent compilation[1] or another source. If the latter is not available, the plot is labeled with 'N/A'. Here, independent $SO_2$ flux data for Lastarria are from [9].

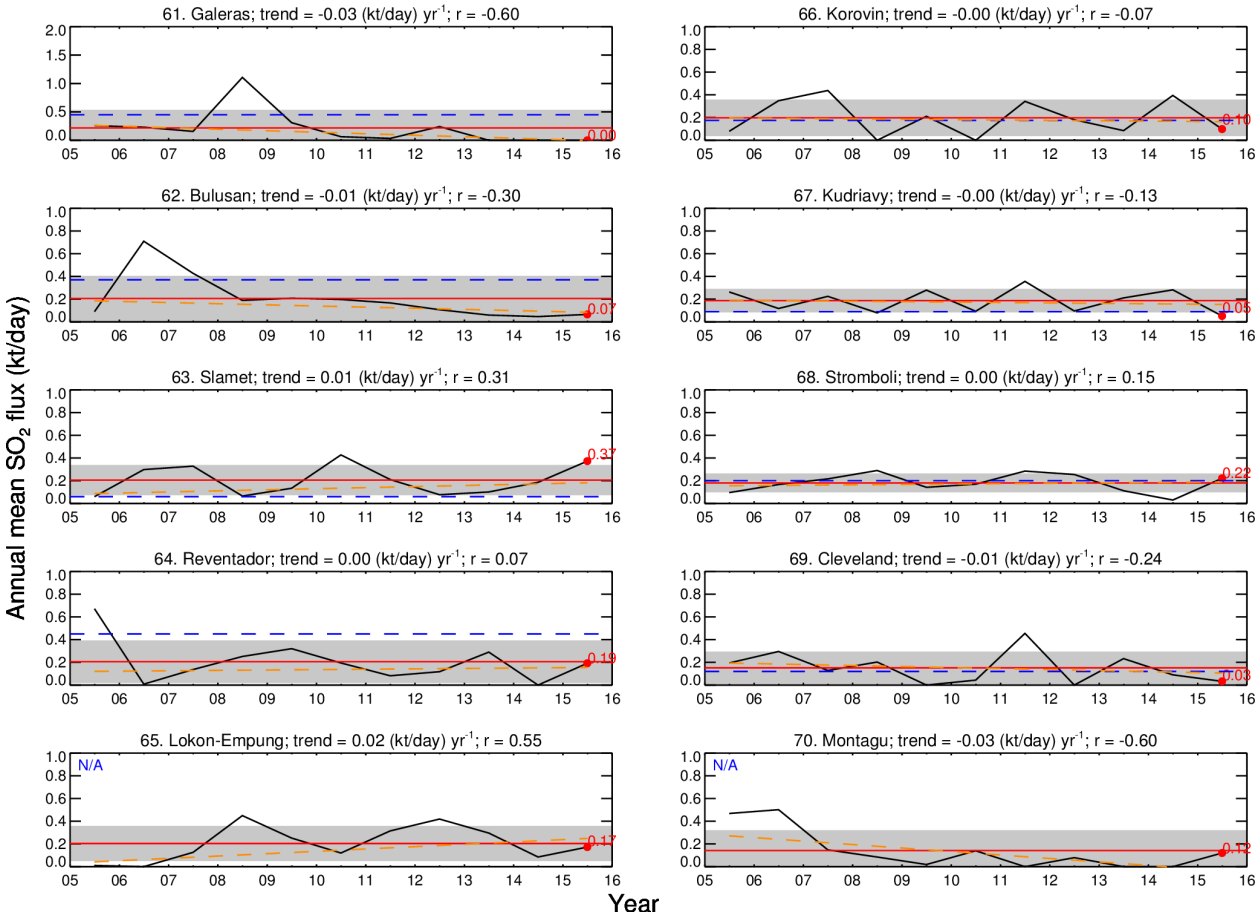


**Figure S14.** OMI-derived annual mean $SO_2$ fluxes in 2005-2015 for the volcanic $SO_2$ sources ranked 61-70 in the inventory. Plots are titled with the volcanic source name and rank, and the trend (slope) and linear correlation coefficient (*r*) of an error-weighted linear regression fit of the annual mean $SO_2$ fluxes. Each plot shows the annual mean $SO_2$ fluxes (*solid black line*), mean $SO_2$ flux in 2015 (*labeled red dot*), linear regression trend line (*dashed orange line*), decadal mean $SO_2$ flux (*horizontal red line*), ±1 standard deviation of the decadal mean $SO_2$ flux (*gray band*), and an independent estimate of $SO_2$ flux (*horizontal dashed blue line*) from a recent compilation[1] or another source. If the latter is not available, the plot is labeled with 'N/A'.

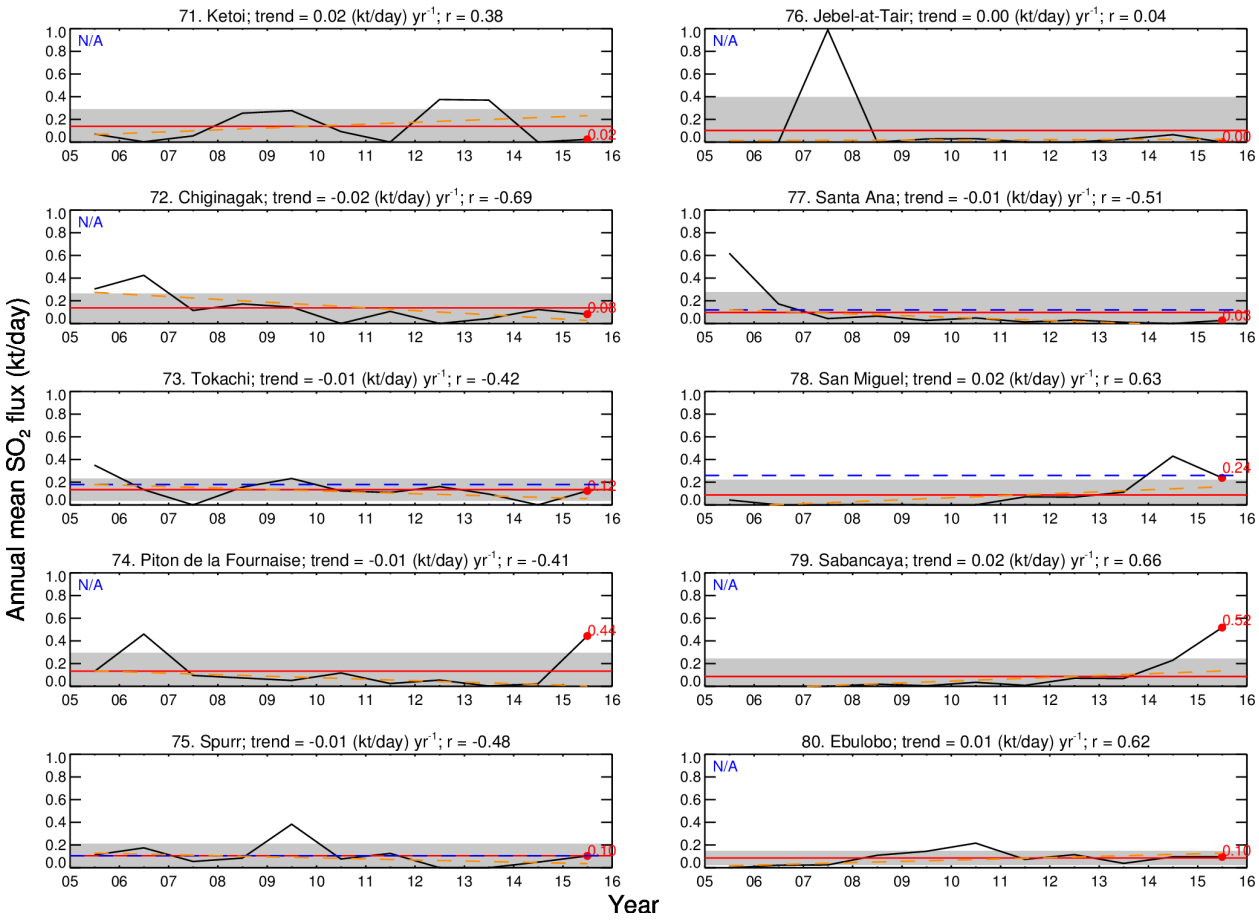


**Figure S15.** OMI-derived annual mean $SO_2$ fluxes in 2005-2015 for the volcanic $SO_2$ sources ranked 71-80 in the inventory. Plots are titled with the volcanic source name and rank, and the trend (slope) and linear correlation coefficient (*r*) of an error-weighted linear regression fit of the annual mean $SO_2$ fluxes. Each plot shows the annual mean $SO_2$ fluxes (*solid black line*), mean $SO_2$ flux in 2015 (*labeled red dot*), linear regression trend line (*dashed orange line*), decadal mean $SO_2$ flux (*horizontal red line*), ±1 standard deviation of the decadal mean $SO_2$ flux (*gray band*), and an independent estimate of $SO_2$ flux (*horizontal dashed blue line*) from a recent compilation[1] or another source. If the latter is not available, the plot is labeled with 'N/A'. Here, independent $SO_2$ flux data for Spurr are from [10].

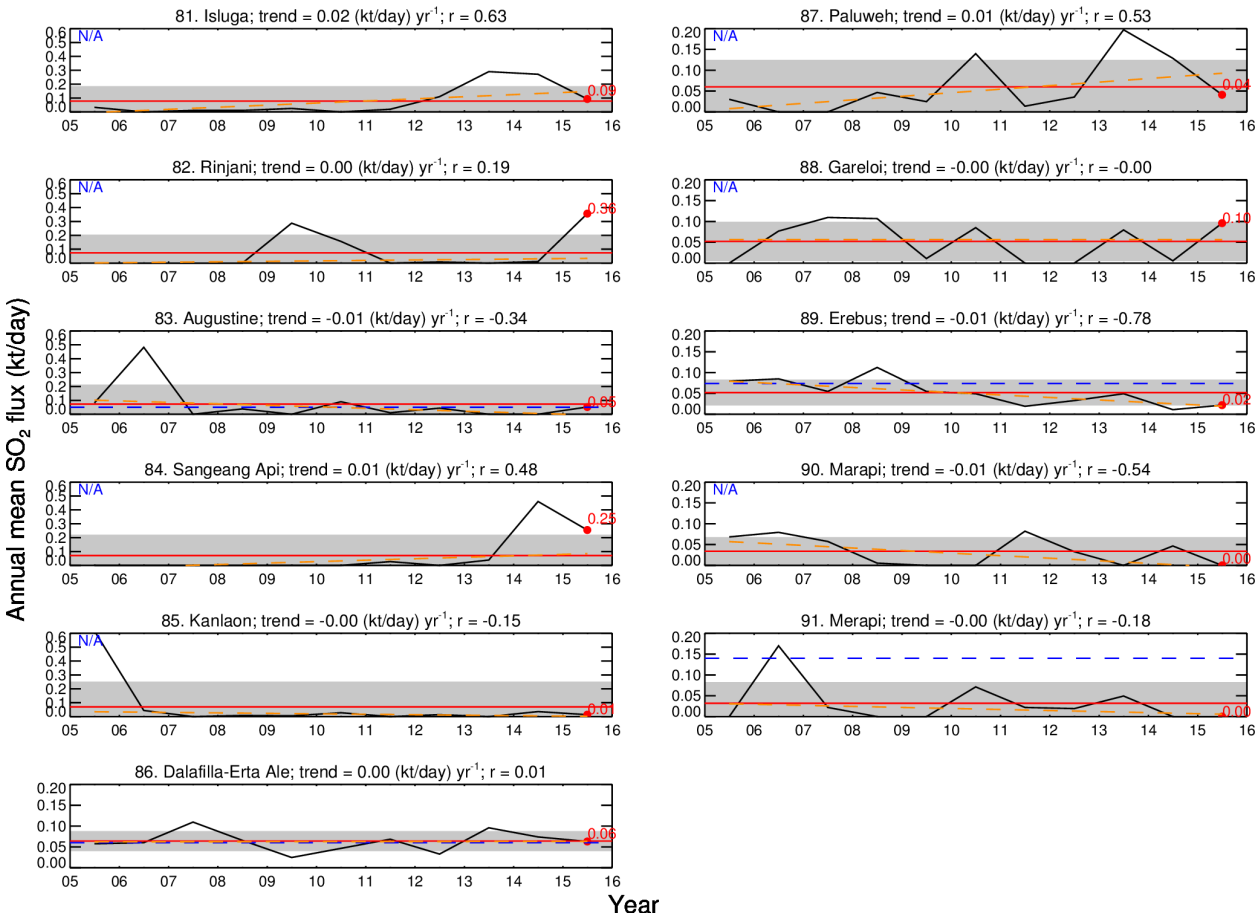


**Figure S16.** OMI-derived annual mean $SO_2$ fluxes in 2005-2015 for the volcanic $SO_2$ sources ranked 81-91 in the inventory. Plots are titled with the volcanic source name and rank, and the trend (slope) and linear correlation coefficient (*r*) of an error-weighted linear regression fit of the annual mean $SO_2$ fluxes. Each plot shows the annual mean $SO_2$ fluxes (*solid black line*), mean $SO_2$ flux in 2015 (*labeled red dot*), linear regression trend line (*dashed orange line*), decadal mean $SO_2$ flux (*horizontal red line*), ±1 standard deviation of the decadal mean $SO_2$ flux (*gray band*), and an independent estimate of $SO_2$ flux (*horizontal dashed blue line*) from a recent compilation[1] or another source. If the latter is not available, the plot is labeled with 'N/A'.

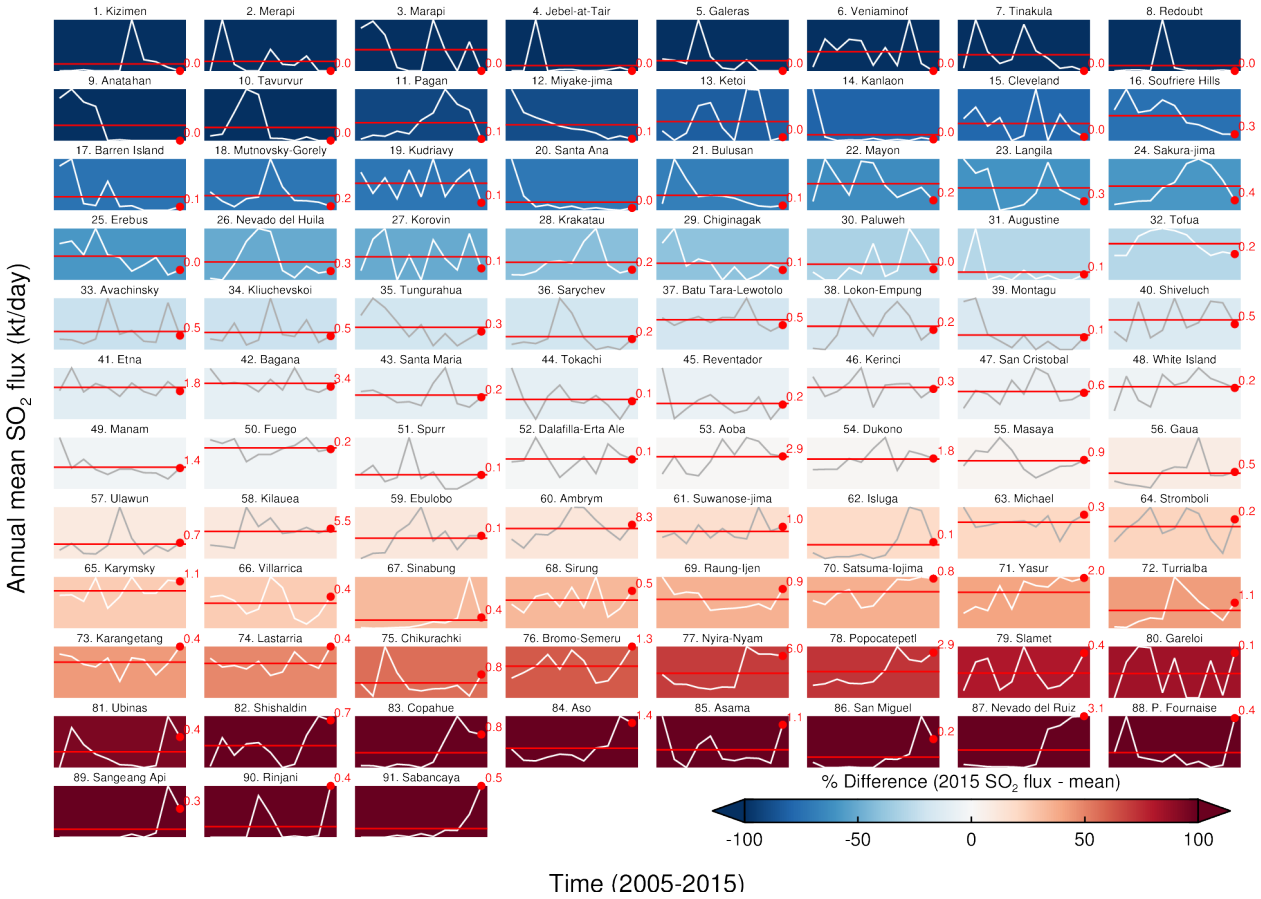


**Figure S17.** Difference between OMI-derived $SO_2$ flux in 2015 and the decadal mean flux measured at all detected volcanic $SO_2$ sources. Plots are ranked in order of % difference between their annual mean $SO_2$ emissions in 2015 and their 2005-2015 decadal mean $SO_2$ flux. Hence, warm and cold colors indicate sources with 2015 $SO_2$ emissions above and below the long-term average, respectively. Each plot shows the annual mean $SO_2$ fluxes for 2005-2015 (*white-gray line*), the decadal mean $SO_2$ flux (*red line*) and the annual mean $SO_2$ flux in 2015 (*labeled red dot*) for each source; axis labels are omitted for clarity. The vertical scale on each plot extends from zero to the maximum measured $SO_2$ flux.

**References**


1. Shinohara, H. Volatile flux from subduction zone volcanoes: Insights from a detailed evaluation of the fluxes from volcanoes in Japan. *J. Volcanol. Geotherm. Res*. **268**, 46-63, doi: 10.1016/j.jvolgeores.2013.10.007 (2013).

2. Hilton, D. R., Fischer, T. P., McGonigle, A. J. S. & de Moor, J. M. Variable $SO_2$ emission rates for Anatahan volcano, the Commonwealth of the Northern Mariana Islands: Implications for deriving arc-wide volatile fluxes from erupting volcanoes. *Geophys. Res. Lett.* **34**, L14315, doi:10.1029/2007GL030405 (2007).

3. Aiuppa, A. *et al.* First determination of magma-derived gas emissions from Bromo volcano, eastern Java (Indonesia). *J. Volcanol. Geotherm. Res*. **304**, 206-213 (2015).

4. Smekens, J.-F., Clarke, A. B., Burton, M. R., Harijoko, A. & Wibowo, H. E. $SO_2$ emissions at Semeru volcano, Indonesia: Characterization and quantification of persistent and periodic explosive activity. *J. Volcanol. Geotherm. Res*. **300**, 121-128, doi: 10.1016/j.jvolgeores.2015.01.006 (2015).

5. Campion, R. *et al*. Space- and ground-based measurements of sulfur dioxide emissions from Turrialba volcano (Costa Rica). *Bull. Volcanol*. **74**(7), 1757–1770 (2012).

6. Bani, P. *et al.* First arc-scale volcanic $SO_2$ budget for the Vanuatu archipelago. *J. Volcanol. Geotherm. Res*. **211-212**, 36–46, http://dx.doi.org/10.1016/j.jvolgeores.2011.10.005 (2012).

7. Werner, C. A. *et al.* Degassing of $CO_2$, $SO_2$, and $H_2S$ associated with the 2009 eruption of Redoubt Volcano, Alaska, 1989–2006. *J. Volcanol. Geotherm. Res*. **259**, 270-284 (2013).

8. Bani, P. *et al.* First measurement of the volcanic gas output from Anak Krakatau, Indonesia. *J. Volcanol. Geotherm. Res*. **302**, 237-241, doi: 10.1016/j.jvolgeores.2015.07.008 (2015).

9. Tamburello, G., Hansteen, T. H., Bredemeyer, S., Aiuppa, A. & Tassi, F. Gas emissions from five volcanoes in northern Chile and implications for the volatiles budget of the Central Volcanic Zone. *Geophys. Res. Lett*. **41**, 4961–4969, doi:10.1002/2014GL060653 (2014).

10. Werner, C. A., Doukas, M. P. & Kelly, P. J. Gas emissions from failed and actual eruptions from Cook Inlet Volcanoes, Alaska, 1989–2006. *Bull. Volcanol*. **73**(2), 155-173 (2011).